Research Article

Experimental Study of the Shear Behavior and Shear Strength of Hybrid Fiber-Reinforced SCC Rectangular Beams

Yunlong Zhou [iD],[1,2] Xiongxiong Liang,[1] Jinjun Kang,[1] and Zhiguo You [iD][1,2,3]

[1]*College of Civil and Architectural Engineering, North China University of Science and Technology, Tangshan 063210, China*
[2]*Earthquake Engineering Research Center of Hebei Province, Tangshan 063210, China*
[3]*Key Laboratory of Building Collapse Mechanism and Disaster Prevention, China Earthquake Administration, Langfang 065201, China*

Correspondence should be addressed to Zhiguo You; youzhiguo@ncst.edu.cn

Based on the investigation on the workability of macro-mono-steel fibers and macro-hybrid fiber-reinforced self-consolidating concrete, a series of simply supported hybrid fiber-reinforced self-consolidating concrete rectangular beams with four-point vertical load were analyzed by using experiments. Influences of steel fibers and hybrid fibers with various dosages on the shear strength and failure mode of reinforced concrete beams are analyzed. This work finds that hybrid fibers can evidently enhance the shear strength. The failure mode of the beam can be changed from a brittle shear failure into a ductile flexural mechanism due to enough hybrid fibers added. The mechanical behavior of the hybrid fiber-reinforced self-consolidating concrete beam is much better than that of macro-mono-steel fiber-reinforced self-consolidating concrete. Hybrid fibers combined with stirrups show the synergistic response and that is a good way of reinforcement for self-consolidating concrete members. The ultimate shear load of beams with hybrid fibers and/or shear reinforcement can be predicted by the σ-w design method suitably.

1. Introduction

Steel fibers (SFs) show outstanding performance in improving the strength and toughness of concrete [1–10]. A reinforced concrete (RC) beam may be subjected to diagonal cracks when the principal tensile stress exceeds its tensile strength. Adding macro-SF into a RC beam enhances the shear strength, which is conductive to a more ductile mechanism if sufficient SFs are added, tending to reduce crack size and spacing [2–4, 9, 10].

Positive hybrid effects on the flexural toughness and crack pattern of beams and slabs may be realized by adding enough hybrid fibers (a combination of macro-SF and macro-PP-fiber) and can enhance the fiber reinforcement [11]. Noghabai [12] evaluated RC beams with hybrid fibers (hybrid macro-SF and micro-SF) under shear and bending and found that hybrid fibers may improve the efficiency of fiber-reinforced concrete (FRC), and RC beams with FRC are competitive with conventional RC beams with stirrups.

However, the research results on shear behavior for hybrid fibers (especially for hybrid macro-SF and macro-plastic fiber (PF)) RC beams are very rare.

The fiber-reinforced self-consolidating concrete (FRSCC) is different from traditional FRC because the fiber dosage of the latter is, to the largest degree, under the determination of post-cracking behavior, and that of the former is restricted due to the workability of SCC [13]. Greenough and Nehdi [14] believed that the shear property of the non-stirrup FRSCC beams was superior to that of traditional FRC beams because the fiber distribution was more uniform. This is mainly due to the better workability of FRSCC and the more efficient elimination of mechanical vibration. FRSCC greatly shortens the period of construction, reduces the cost, and reduces the reinforcement strength. In addition, FRSCC beams are presented with thin or irregularly shaped sections, where it may be very difficult to place stirrups. Analyzing FRSCC is a current developing trend because it integrates the advantages of both SCC and

FRC. Until now, there have been only a few investigations on the influence of hybrid fibers on workability.

In the previous stage, the research group studied the shear resistance of hybrid fiber-reinforced SCC T-beams, analyzed the effects of fiber dosage, stirrup ratio, and flange size on the shear capacity, and established the shear capacity formula of T-beams in [22]. Due to the flanges in T-beam, the shear performance of rectangular beams is different from that of T-beam when the fiber and stirrups work together. In the conference paper [23] published by our group, the experimental results of the influences of steel fibers and hybrid fibers on the ultimate shear load and failure mode of rectangular beams were only simply analyzed. In this paper, the same batch of test beams is used, but more detailed experimental design, result, analysis, and theoretical research are carried out. Based on the slump flow test and J-ring test for measuring the workability of SCC with fibers, the results and analysis on the shear behavior of mono-fiber and hybrid fiber-reinforced SCC rectangular beams are presented. The "revised σ-w design method" and the "revised σ-ε design method" are employed to predict the ultimate shear load of hybrid fiber-reinforced SCC or steel fiber-reinforced SCC beams.

2. Test Program

2.1. Beam Geometry and Setup Description.
A series of hybrid fiber-reinforced SCC beams (ten beams) were experimentally studied. The beam out of the experimental zone (collapse location) is stiffened to get a shear failure in a half beam (experimental zone) and systematic measurements on the displacement and strain of shear span. The stirrup ratio of every rectangular beam out of the experimental zone is larger compared with that in the experimental zone.

The parameters of the beams are given in Table 1. Each beam is nominated to show the stirrup spacing and steel fiber and plastic fiber dosages. BSS150SF20PF6 contains the SF dosage of 20 kg/m^3, PF dosage of 6 kg/m^3, and a stirrup spacing of 150 mm. The first, second, and third numbers indicate the stirrup spacing, the SF dosage, and the PF dosage, respectively.

The beam dimension is B (width) $\times$ H (depth) $\times$ L (length) = 125 $\times$ 250 $\times$ 1750 mm, tested on a span L_s = 1500 mm. Two stirrup ratios and four fiber dosages are employed to explore and analyze the effects of fiber dosage on the shear behavior of hybrid fiber-reinforced SCC beams. According to GB 50010-2010 (Chinese code) [15], the two stirrup ratios are 0.35% and 0.53%, respectively, which are greater than the minimum stirrup ratio. On account of the workability of fresh SCC, the fiber dosages are chosen as 20.0 kg/m^3 (SF), 20.0 + 6.0 kg/m^3 (SF + PF), 40.0 kg/m^3 (SF), and 40.0 + 4.0 kg/m^3 (SF + PF). The shear span-to-depth ratio (a/d = 3.2) and longitudinal reinforcement ratio ρ_s = 3.38% (diameter 25 mm, 2 longitudinal reinforcements) are kept constant. The geometry and reinforcement details of rectangular beams can be seen in Figure 1.

The loading and measuring arrangement of the beam is shown in Figure 2. The beams are subjected to the symmetrically concentrated two-point loading. Strain gauges are fixed on the longitudinal reinforcement at the midspan load point and 212.5 mm far away from the support for the purpose of evaluation of the influence of fibers on the strain. In addition, the linear variable differential transformers (LVDTs) were selected to measure the beam displacement at the midspan, load points, and support. The capacity of the test machine is 10000 kN. Load transducer with 500 kN is set to measure the load. The beam displacement at midspan increases at 0.2 mm/min until a stipulated load in accordance with the Chinese Code for Test Methods of Concrete Structures (GB50152-92) [16]. The above stated specified load should be constant until the measured LVDT and strain are stable. During the test, the load and displacement are recorded all the time.

2.2. Material Properties.
The SCC is composed of Portland cement 42.5R, fly ash, fine aggregate, coarse aggregate, superplasticizer, and water, the detailed proportions of which are listed in Table 2. The maximum gravel size is 10.0 mm. The SF and PF are mixed in the SCC. For SF(RC-65/35-BN), the fiber length (Lf) and equivalent diameter (Df) are 35 mm and 0.55 mm, respectively, so Lf/Df = 65, and the nominal tensile strength is 1150 MPa, while for PF, values of the above three indicators are 30 mm, Df = 0.66 mm (Lf/Df = 45), and 780 MPa, respectively.

The yield stress of the longitudinal reinforcement and stirrup is 466 MPa and 354 MPa, respectively, and the ultimate stress of them is 654 MPa and 527 MPa, respectively.

2.3. Test Methods of Workability.
The workability of fresh SCC can be evaluated according to references [17–19]. A concrete mix has to meet the specific requirements for the workability of flowability, segregation resistance, passing ability, filling ability, and leveling ability before it is called as SCC. The slump flow test (for assessing the workability and filling ability) and J-ring test (for assessing passing ability, flowability, and segregation resistance) are employed for the production quality control in this paper (Figure 3) [17–19].

Figure 3 illustrates the test of workability of SCC with 20 kg/m^3 SF + 6 kg/m^3 PF and that of SCC with 40 kg/m^3 SF +6 kg/m^3 PF. The results suggested that the workability of the fiber-reinforced fresh mixture with the dosage of 20 kg/m^3 SF + 6 kg/m^3 PF fulfills the requirement of SCC [17–19], but that of the fiber-reinforced fresh mixture with the dosage of 40 kg/m^3 SF + 6 kg/m^3 PF cannot fulfill the requirement.

2.4. Test Methods of Flexural Strength and Toughness.
In order to evaluate the flexural strength and toughness of hybrid fiber-reinforced SCC based on matrix mix proportion, 6 test pieces with the size 150 mm $\times$ 150 mm $\times$ 550 mm shall be prepared for each kind of hybrid fiber-reinforced SCC. The test shall be carried out after 28 days of curing as specified in "RILEM TC 162-TDF." All test beams are loaded by a 1000 kN hydraulic servo testing machine with constant speed displacement closed-loop control, and the midspan displacement rate is 0.2 mm/min. Two LVDTs and crack gauges are used on both sides and bottom of the beam to

TABLE 1: The parameters of beam.

| Beam no.	Beam width (mm)	Effective depth (mm)	Testing zones			SF dosage ($kg \cdot m^{-3}$)	PF dosage ($kg \cdot m^{-3}$)
			Stirrup diameter (mm)	Stirrup space (mm)	Stirrup ratio		
BSS∞SF0PF0	125	212.5	0	∞	0	0	0
BSS∞SF20PF0	125	212.5	0	∞	0	20	0
BSS∞SF20PF6	125	212.5	0	∞	0	20	6
BSS∞SF40PF0	125	212.5	0	∞	0	40	0
BSS∞SF40PF4	125	212.5	0	∞	0	40	4
BSS150SF0PF0	125	212.5	6.5	150	0.35%	0	0
BSS150SF20PF6	125	212.5	6.5	150	0.35%	20	6
BSS150SF40PF0	125	212.5	6.5	150	0.35%	40	0
BSS150SF40PF4	125	212.5	6.5	150	0.35%	40	4
BSS100SF0PF0	125	212.5	6.5	100	0.53%	0	0

(a)

(b)

(c)
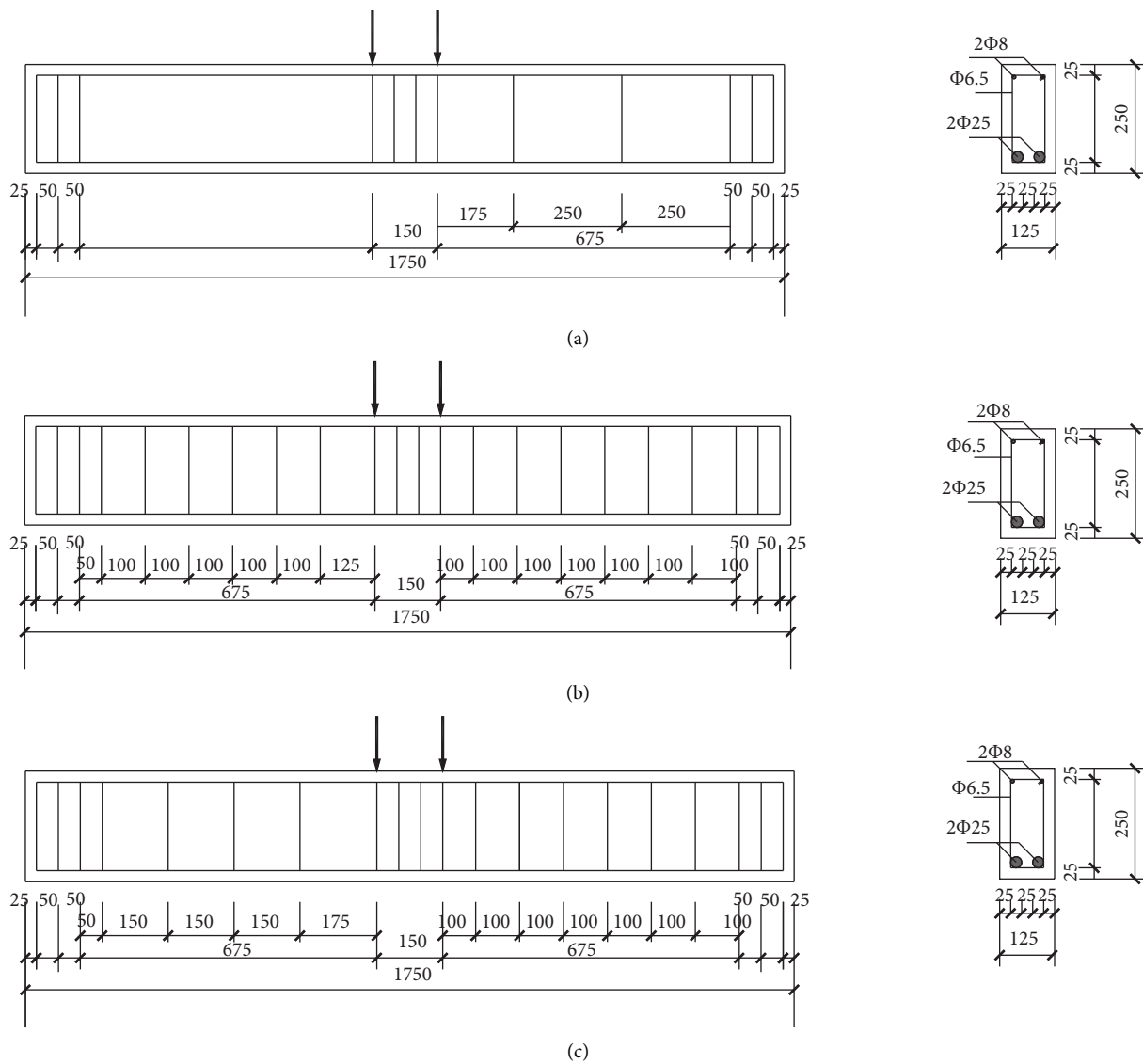
FIGURE 1: Geometry and reinforcement details of rectangular beams. (a) Stirrup ratio 0% (without stirrup). (b) Stirrup ratio 0.53% (SS100). (c) Stirrup ratio 0.35% (SS150).
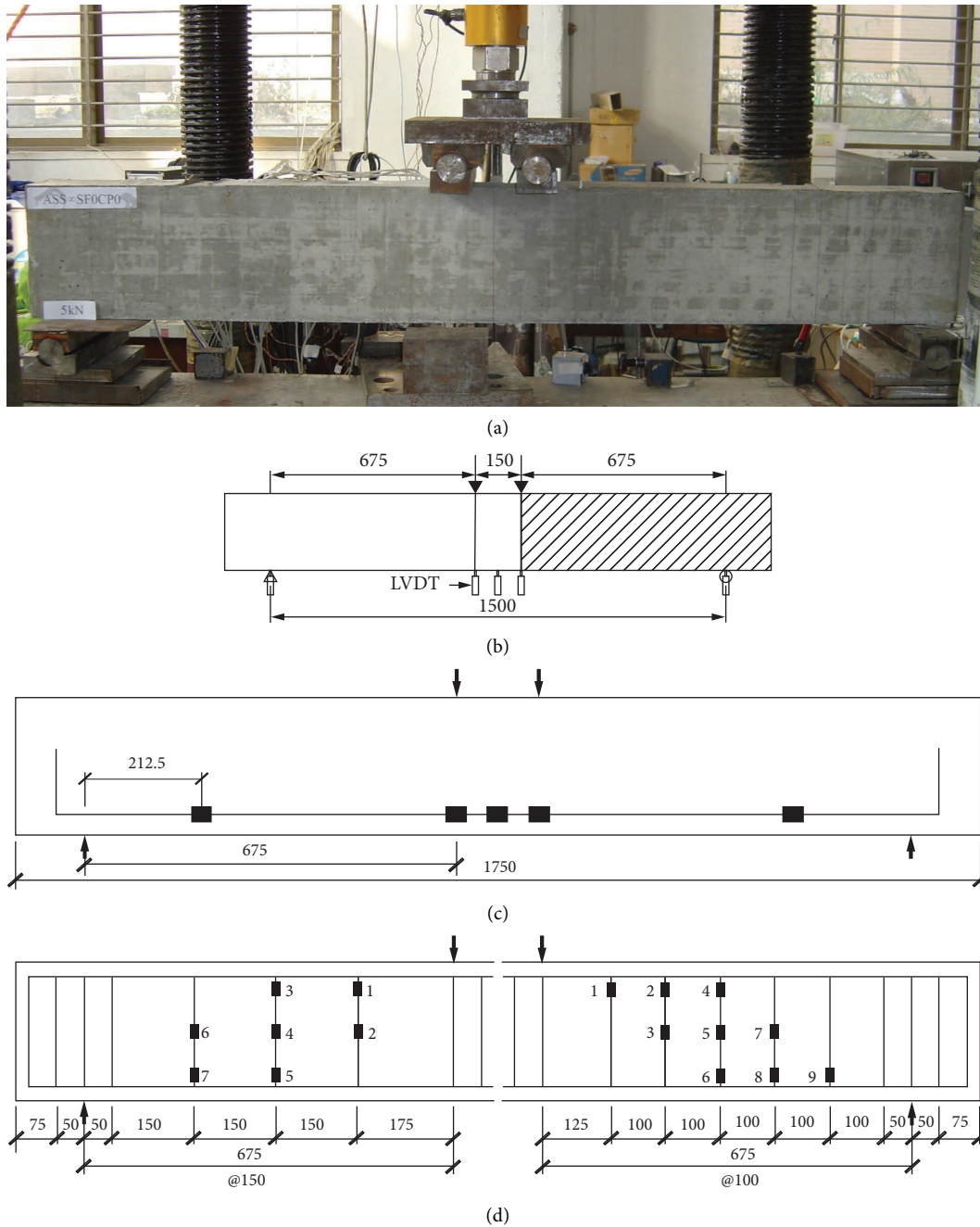
(a)

(b)

(c)

(d)

FIGURE 2: Loading and measuring system. (a) Loading mode. (b) LVDT arrangement. (c) Bottom load-bearing reinforcement strain gauge. (d) Stirrup strain gauge.

TABLE 2: Mix proportion design.

Cement (kg·m^{-3})	Fly ash (kg·m^{-3})	Water (kg·m^{-3})	Fine aggregate (kg·m^{-3})	Coarse aggregate (kg·m^{-3})	Superplasticizer (%)	W/B (%)
388	166	210	769	710	0.9–1.2	0.38

measure the midspan deflection and crack mouth open displacement of the beam separately. Also, the average value of the two LVDTs is taken during the calculation to eliminate the influence of the torsion of the beam. The test apparatus is shown in Figure 4.

3. Results

3.1. Test Results of Workability and Cubic Compressive Strength. The workability of hybrid fiber-reinforced SCC is listed in Table 3, and the experimental results are obtained
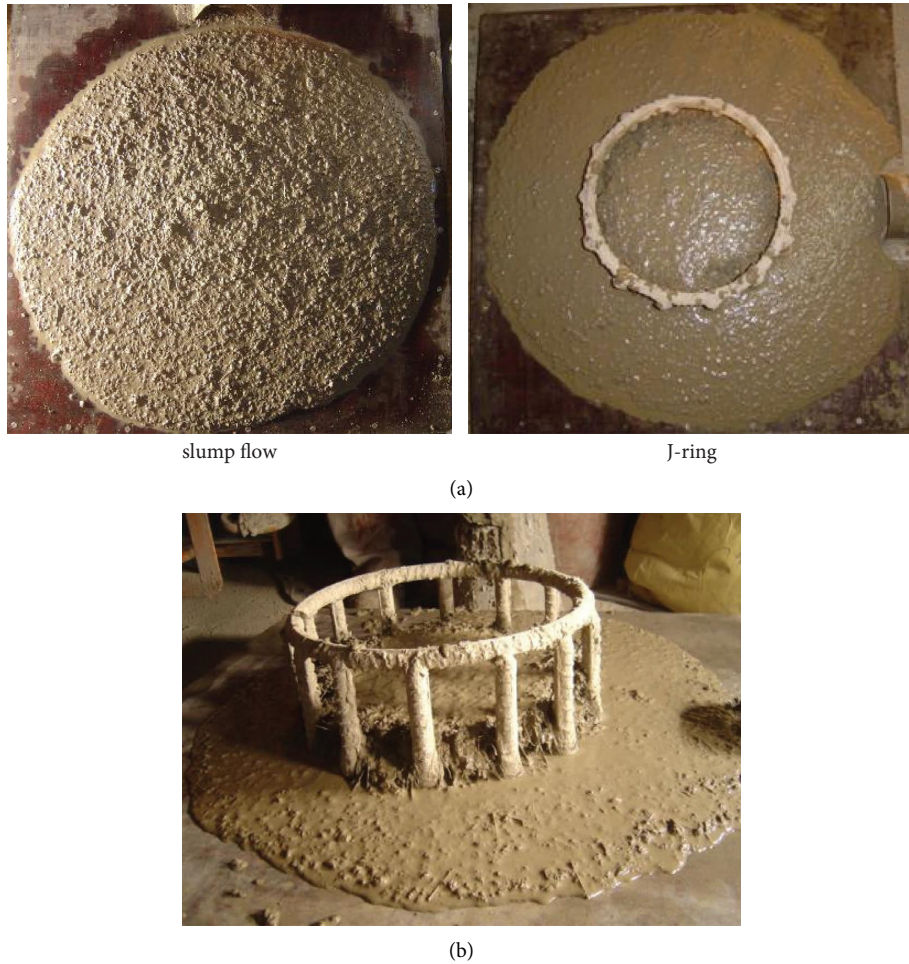
slump flow   J-ring

(a)

(b)

FIGURE 3: The workability of self-consolidating concrete with 20 kg/m^3 SF + 6 kg/m^3 PF and 40 kg/m^3 SF and 6 kg/m^3 PF. (a) SF dosage of 20 kg/m^3 and PF dosage of 6 kg/m^3. (b) J-ring of Self-consolidating concrete with SF dosage of 40 kg/m^3 and PF dosage of 6 kg/m^3.
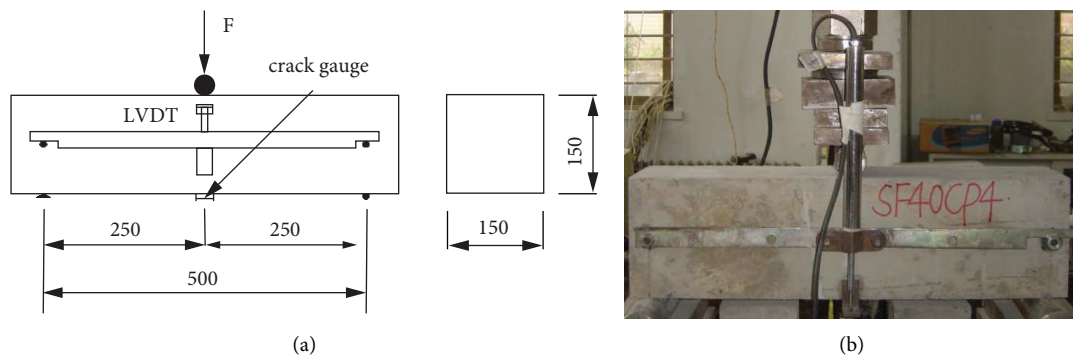

(a)   (b)

FIGURE 4: Flexural test of hybrid fiber-reinforced SCC beams. (a) Test design. (b) Test device.

from the average values of six specimens. Factor d represents the average final diameter of the concrete in two perpendicular directions in the slump flow test or J-ring test. Factor T_{500} refers to the time for the concrete to reach the specific spread circle (500 mm). Factor h is the average height difference between the concretes inside and outside the bars at four locations in the J-ring test.

Workability of hybrid fiber-reinforced SCC in Table 3 tells us that all parameters except SF40PF6 can meet the European Federation of National Associations Representing for Concrete (EFNARC) [17–19]. When the hybrid fiber dosage is 40 + 4 kg/m^3, the height is 15 mm between the inside steel rebar and the outside one in the J-ring test, satisfying the required $h \leq 15$ mm [17–19]. The average

TABLE 3: Test results of workability and cubic strength.

Fiber type (kg·m⁻³)	Slump flow		J-ring		Cubic strength
	d (mm)	T_{500} (s)	d (mm)	h (mm)	f_{cu} (MPa)
SF0PF0	780	3.0	780	1	47.71
SF20PF0	770	3.3	740	2	46.62
SF20PF6	740	4.1	700	10	49.07
SF40PF0	760	3.8	730	8	33.73
SF40PF4	730	4.5	700	15	36.03
SF40PF6	700	5.0	660	20	—

SF20PF6 means the FRSCC with the dosage of 20 kg/m³ SF and 6 kg/m³ PF.

height difference between the concrete just inside and outside the bars at four locations in the J-ring test is 20 mm, failing to satisfy the requirement (Table 3 and Figure 2(b)). Therefore, it can be concluded that the beam with hybrid fiber dosage of $40 + 4$ kg/m³ could satisfy to achieve the upper limit of the workability of FRSCC. The dimension of casted cubic specimens is $150 \times 150 \times 150$ mm. Table 3 lists the cubic compressive strength f_{cu} at the time of testing. Adding fibers aids in converting the brittle properties of concrete into a ductile material, but the improvement of the compressive strength is not obvious.

3.2. Shear Load-Displacement Curves

3.2.1. Shear Load-Displacement Curves of Beams without Stirrups. Figure 5 compares the shear load-displacement curves (F-Δ curves) of the beams without stirrup (stirrup ratio = 0%). Table 4 lists the ultimate shear load and the ultimate displacement at the load point and failure mode.

The following contents can be observed from Table 4 and Figure 5:

The specimen BSS∞SF0PF0 (without stirrups, without fibers) shows lower load bearing capacity ($F_u = 42.72$ kN) and brittle failure mode failing in shear collapse. After application of the ultimate shear load F_u, no post-peak behavior is found for the beam BSS∞ SF0PF0, and the load bearing capacity declines sharply. Compared with the specimen BSS∞SF0PF0, the load bearing capacities of BSS ∞ SF20PF6 and BSS ∞ SF40PF4 are much higher during the displacement. The displacement at the load point of the hybrid fiber-reinforced SCC beams decreases under the same load before the peak load of beam. The stiffness of the hybrid fiber-reinforced SCC beams increases obviously due to the fiber delaying cracks, restricting further cracks [20]. The ultimate shear load F_u and the UD (ultimate displacement) Δ_u corresponding to F_u at the load point of the hybrid fiber-reinforced SCC beams increase. It can be concluded that adding hybrid fibers enhances the toughness greatly and alters the crack pattern from the strong brittleness of the beam BSS∞SF0PF0 into a relatively ductile one (more cracks and minor crack space) of specimen BSS∞SF20PF6 or BSS∞SF40PF4, although the failure mode of the two beams is shear collapse.

Compared with the specimen BSS ∞ SF20PF0 (containing 20 kg/m³ mono-SF, without stirrups), the specimen BSS ∞ SF20PF6 (stirrup ratio = 0%) in the pre-peak region shows a decreased displacement at the load point with the same load, and its stiffness increases significantly. The ultimate shear load F_u of the specimen BSS ∞ SF20PF6 increases by almost 25%, and UD Δ_u corresponding to F_u at the load point decreases by just 2%, but the fiber dosage increases by almost 30%. The specimen BSS ∞ SF20PF6 shows a better post-peak load bearing capacity than the BSS ∞ SF20PF0.

Compared with the beam BSS ∞ SF40PF0 (containing 40 kg/m³ mono-SF, without stirrups), no significant difference is observed in the displacement of the specimen BSS ∞ SF40PF4 (containing 40 kg/m³ SF and 4 kg/m³ PF, without stirrups). The ultimate shear load of the specimen BSS ∞ SF40PF4 and UD Δ_u at the load point increase by 27.89% and 28.81%, respectively, while the fiber dosage increases by only 10%. The specimen BSS ∞ SF40PF4 exhibits a much better post-peak load bearing capacity than the specimen BSS ∞ SF40PF0.

Compared with the beam BSS ∞ SF40PF0 (containing 40 kg/m³ mono-SF, without stirrups), no significant difference is found in the displacement of the beam BSS ∞ SF20PF6 (stirrup ratio = 0%) when the load is constant before the peak load. Both the ultimate shear load and the UD Δ_u at the load point of the beam BSS ∞ SF20PF6 increase by about 10.8%, while the fiber dosage decreases by almost 35%. The post-peak load bearing capacity of the beam BSS ∞ SF20PF6 is significantly improved compared to the post-peak load bearing capacity of BSS ∞ SF40PF0.

The F-Δ curves among BSS ∞ SF20PF6, BSS ∞ SF40PF4 (hybrid SF and PF), and BSS ∞ SF40PF0 (with mono-SF) demonstrate better load bearing capacity and deformability and potential cost benefit of applying hybrid fibers. It clearly exhibits that the efficiency of the hybrid mixture is high and the synergistic effect among the fibers is obvious.

3.2.2. Shear Load-Displacement Curves of Beams with Stirrups. Figure 6 compares the F-Δ curves of the beams with stirrups (stirrup ratio of 0.35% and 0.53%).

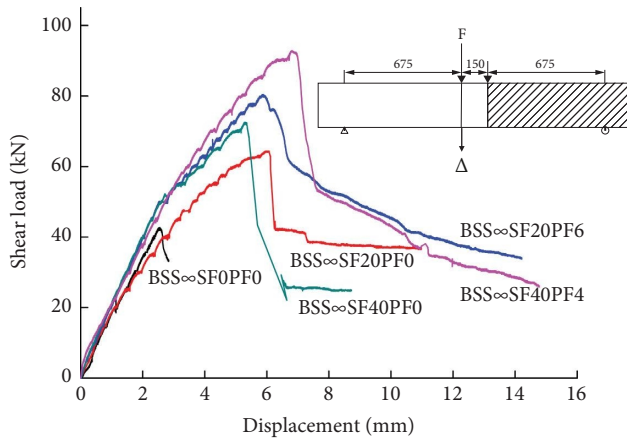The following results can be observed from Table 4 and Figure 6:

FIGURE 5: Shear load-displacement curves of the beams with different fiber types and without stirrups.

Compared with the specimen BSS150SF0PF0 (with a stirrup ratio of 0.35%, without fibers), the displacement at the load point of the hybrid fiber-reinforced SCC beams (beams BSS150SF20PF6 and BSS150SF40PF4) decreases when the load is not changed before the peak load. It means that the stiffness of the hybrid fiber-reinforced SCC beams increases marginally. The load bearing capacity of the hybrid fiber-reinforced SCC beams behaves obviously better compared to that of BSS150SF0PF0 during the displacement. The ultimate shear load of the hybrid fiber-reinforced SCC beams increases significantly. The UD (ultimate displacement) Δ_u of the beam BSS150SF20PF6 at the load point increases appreciably. $40 + 4 \, \text{kg/m}^3$ hybrid fibers transform the brittle shear failure mode of BSS150SF0PF0 into a ductile flexure mechanism of the specimen BSS150SF40PF4.

Compared with the specimen BSS150SF40PF0 (both with $40 \, \text{kg/m}^3$ mono-SF and a stirrup ratio of 0.35%), adding $40 + 4 \, \text{kg/m}^3$ hybrid fibers into BSS150SF0PF0 enhances the ultimate shear load by 1.5% at least.

Compared with the specimen BSS150SF40PF0 (both with $40 \, \text{kg/m}^3$ mono-SF and a stirrup ratio of 0.35%), the ultimate shear load of the specimen BSS150SF20PF6 decreases by 6.3%, and the UD Δ_u at the load point is increased by 5.7% only, while the fiber dosage decreases by almost 35%. The post-peak load bearing capacity of the specimen BSS150SF40PF0 is better in contrast to that of the beam BSS150SF20PF6. Such result is different from the beams BSS∞SF40PF0 and BSS∞SF20PF6 without stirrups but mixed with the same fibers. Maybe the shear capacity of the beam improved is similar or the composite effect of fibers and stirrups on the shear capacity is different from beams with only fibers. More experiments will be done to deeply analyze it.

Compared with the specimen BSS100SF0PF0 (with a stirrup ratio of 0.53%, without fibers), the load bearing capacity during the displacement and the UD Δ_u of

BSS150SF20PF6, BSS150SF40PF0, and BSS150SF40PF4 are better than those of BSS100SF0PF0.

Therefore, the following views are obtained:

(1) The F-Δ curves between beams BSS150SF40PF0 (mono-SF) and BSS150SF40PF4 (hybrid SF and PF) demonstrate better load bearing capacity and deformability of using hybrid fibers.

(2) The F-Δ curves between beams BSS150SF40PF0 (mono-SF) and BSS150SF20PF6 (hybrid SF and PF) demonstrate similar load bearing capacity, better deformability, and possible cost benefit of using hybrid fibers.

(3) The hybrid mixture is higher, and the synergistic effect among the fibers is obvious.

3.3. Failure Mode and Crack Pattern. The cracks occur in the tensile zone of midspan of the beam first, and then the flexural shear cracks occur in the shear span of the beam with increasing load. Table 5 lists the crack characteristics of the shear span of beams, including crack spacing, the maximum crack width W_{max} before the shear collapse, and the maximum crack width W_{60} when the shear load is 60 kN. The crack patterns and failure mode of BSS ∞ SF0PF0 and BSS ∞ SF40PF4 are demonstrated in Figure 7, while those of beams BSS150SF0PF0 and BSS150SF40PF4 are illustrated in Figure 8.

The specimen BSS ∞ SF0PF0 fails after the first diagonal crack forms (Figure 7(a)). UDΔ_u at the load point corresponding to the ultimate shear load is only 2.55 mm (Table 4). The maximum crack width W_{max} before shear collapse is only 0.10 mm (Table 5). The beam BSS ∞ SF0PF0 fails in shear collapse.

Compared with the beam BSS ∞ SF0PF0, the crack pattern is improved after the addition of stirrups and fibers, which can be found by the increase of ultimate displacement Δ_u and number of cracks, the decrease of crack spacing, and the maximum crack width (Tables 4 and 5 and Figures 7 and 8). The hybrid fiber-reinforced SCC beams are far less catastrophic compared to those containing no fibers. For instance, for BSS ∞ SF40PF4, several diagonal cracks were formed and can be observed, the crack spacing and crack width under the same load and before failure declined clearly compared to the other beams without stirrups (Table 5 and Figure 7(b)). It suggests that adding some fibers can make the stress redistribution more even over the cracks. The SFs are effective after the occurrence of diagonal cracking before they are completely pulled out at the critical crack. The PFs are partly pulled out and broken down. This observation supports the use of hybrid fibers in SCC, and hybrid fibers can effectively protect the further pulling out of the SF from the concrete matrix after they are cracked (Figure 9).

Addition of $40 + 4 \, \text{kg/m}^3$ hybrid fibers transforms the failure mode of BSS150SF0PF0 from brittle shear collapse (Figure 8(a)) to flexural failure mode (Figure 8(b)). The BSS150SF40PF4 exhibits a crushed compression zone (Figure 8(b)), except which all beams fail in shear collapse.

TABLE 4: Ultimate shear load and ultimate displacement at load point.

| Beam no.	Beam width (mm)	Effective depth (mm)	Testing areas			Steel fiber dosage (kg·m^{-3})	Plastic fiber dosage (kg·m^{-3})	Ultimate shear load F_u (kN)	Ultimate displacement at loading point Δ_u (mm)	Failure mode
			Stirrup diameter (mm)	Stirrup space (mm)	Stirrup ratio					
BSS∞SF0PF0	125	212.5	0	∞	0	0	0	42.72	2.55	Shear failure
BSS∞SF20PF0	125	212.5	0	∞	0	20	0	64.58	5.96	Shear failure
BSS∞SF20PF6	125	212.5	0	∞	0	20	6	80.70	5.85	Shear failure
BSS∞SF40PF0	125	212.5	0	∞	0	40	0	72.86	5.28	Shear failure
BSS∞SF40PF4	125	212.5	0	∞	0	40	4	93.17	6.80	Shear failure
BSS150SF0PF0	125	212.5	6.5	150	0.35%	0	0	98.03	6.91	Shear failure
BSS150SF20PF6	125	212.5	6.5	150	0.35%	20	6	115.14	7.95	Flexure-shear failure
BSS150SF40PF0	125	212.5	6.5	150	0.35%	40	0	122.87	7.52	Flexure-shear failure
BSS150SF40PF4	125	212.5	6.5	150	0.35%	40	4	>124.74	—	Flexure failure
BSS100SF0PF0	125	212.5	6.5	100	0.53%	0	0	111.17	7.24	Shear failure
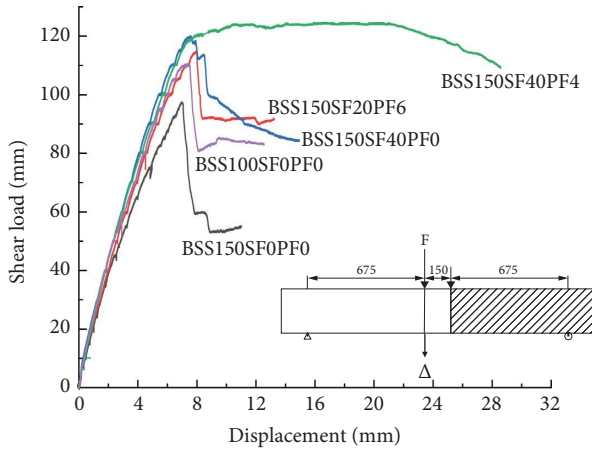
FIGURE 6: Shear load-displacement curves of the beams with different fiber types and stirrups.

3.4. Shear Strength.

The influence of the hybrid fiber on the shear strength $v_u = F_u/bd$ is shown in Figure 10, based on which the following views can be obtained:

The hybrid fiber can affect the shear strength v_u, which is similar to that of the ultimate shear load F_u (Table 3).

When the stirrup ratio is 0%, the shear strength of reinforced concrete beams with fibers of 20.0 kg/m^3, 21 + 6 kg/m^3, 40.0 kg/m^3, and 40 + 4 kg/m^3 increases by 50.99%, 89.00%, 70.53%, and 117.90% compared to BSS ∞ SF0PF0, respectively.

When the stirrup ratio is 0.35%, compared to BSS150SF0PF0, the shear strength of reinforced concrete beams with fibers of 20 + 6 kg/m^3 and 40.0 kg/m^3 is improved by 17.44% and 25.35%, separately. BSS150SF40PF4 fails in flexure. If the flexural capacity of the beam controlled the maximum shear, the applied load at failure cannot be equal to the shear strength; in contrast, the load at failure only limits the lower bound of the shear strength. The shear strength of beam

BSS150SF40PF4 increases at least by 25.22% compared to that of the beam BSS150SF0PF0.

Based on the discussion above, the fiber can affect the shear strength of the beam without stirrup more obviously compared with that of the one with stirrup.

3.5. Ultimate Shear Load of Hybrid Fiber-Reinforced SCC Beams

3.5.1. RILEM TC 162-TDF σ-ε Design Method.
The ultimate shear load of a beam with stirrup and steel fibers according to RILEM TC 162-TDF σ-ε [21] design method is given by the following expression:

$$V_{Rd,3} = V_{cd} + V_{fd} + V_{wd.} \tag{1}$$

V_{cd} is the ultimate shear load of the member without shear reinforcement, given by

$$V_{cd} = \left[0.12k\left(100\rho_s f_{fck}\right)^{\frac{1}{3}} + 0.15\sigma_{cp} \right] b_w d. \tag{2}$$

V_{fd} is the contribution of the steel fiber shear reinforcement, given by

$$V_{fd} = 0.7k_f k_l \tau_{fd} b_w d. \tag{3}$$

V_{wd} is the contribution of the shear reinforcement due to stirrups and/or inclined bars, given by

$$V_{wd} = \frac{A_{sw}}{s} 0.9\, d f_{ywd} \left(1 + \cot \alpha\right)\sin a. \tag{4}$$

#### 3.5.2. RILEM TC 162-TDF σ-w Design Method.
The ultimate shear load of a beam with stirrup and steel fibers according to RILEM TC 162-TDF σ-w [21] design method is expressed

TABLE 5: Crack characteristics of shear span of beams.

Beam no.	Crack spacing (kN)	W_{max} (mm)	W_{60} (mm)
BSS∞SF0PF0	70~110	0.10	—
BSS∞SF20PF0	70~110	2.50	2.00
BSS∞SF20PF6	20~70	1.65	0.80
BSS∞SF40PF0	70~110	1.50	0.95
BSS∞SF40PF4	30~100	1.25	0.15
BSS150SF0PF0	40~110	1.35	0.35
BSS150SF20PF6	20~100	1.30	0.10
BSS150SF40PF0	10~70	1.35	0.10
BSS100SF0PF0	30~70	0.50	0.10

W_{max} is the maximum crack width before shear failure. W_{60} is the maximum crack width when the shear load is 60 kN.
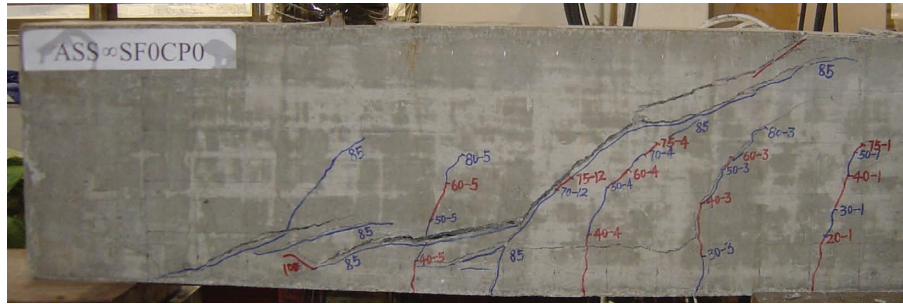
(a)
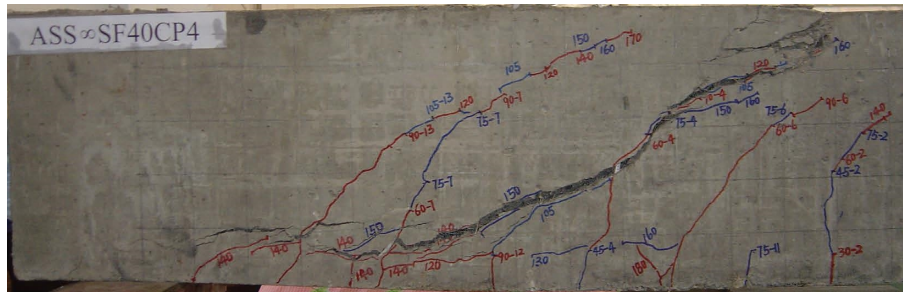
(b)

FIGURE 7: Crack pattern and shear failure of beams BSS ∞ SF0PF0 and BSS ∞ SF40PF4. (a) Shear failure and crack pattern of beam BSS ∞ SF0PF0. (b) Shear failure and crack pattern of beam BSS ∞ SF40PF4.

as (1), too. The difference lies in calculating the contribution of the steel fiber shear reinforcement. In the σ-w design method, it is determined from the design stress-crack opening relationship $\sigma_{w,d}(w)$:

$$V_{fd} = b_w z \overline{\sigma}_{p,d}(w_m),\qquad(5)$$

with

$$\overline{\sigma}_{p,d}(w_m) = \frac{1}{w_m}\int_0^{w_m}\sigma_{w,d}(u)du,\qquad(6)$$

where $\overline{\sigma}_{p,d}(w_m)$ refers to the mean design residual stress at the crack width w_m and denotes the mean value of the post-cracking stress between zero and crack width w_m.

3.5.3. Ultimate Shear Load of Hybrid Fiber-Reinforced SCC Beams.
No equations forecast the ultimate shear load of hybrid fiber-reinforced SCC beams. Thereby, the ultimate shear load of a beam having hybrid fibers and/or with shear

reinforcement can be calculated with reference to Sections 3.5.1 and 3.5.2.

When the ultimate shear load is calculated using the σ-w and σ-ε design methods, the load-deflection curve of the hybrid fiber-reinforced SCC employing notched beam test should be known, which is exhibited in Figure 11. The flexural strength and toughness of hybrid fiber-reinforced SCC are demonstrated in Table 6.

The tensile stress-crack opening relationship of hybrid fiber-reinforced SCC is determined by inverse analysis using the load versus crack mouth opening displacement curve from the notched beam test according to RILEM TC 162-TDF [21] σ-w design method. Because the load-deflection curves of the notched beam are proportional to the load versus crack mouth opening displacement curve, the tensile stress-crack opening relationship of hybrid fiber-reinforced SCC can be determined by inverse analysis using the load-deflection curves of the notched beam. The bilinear stress-crack opening relationship is illustrated in Figure 12.
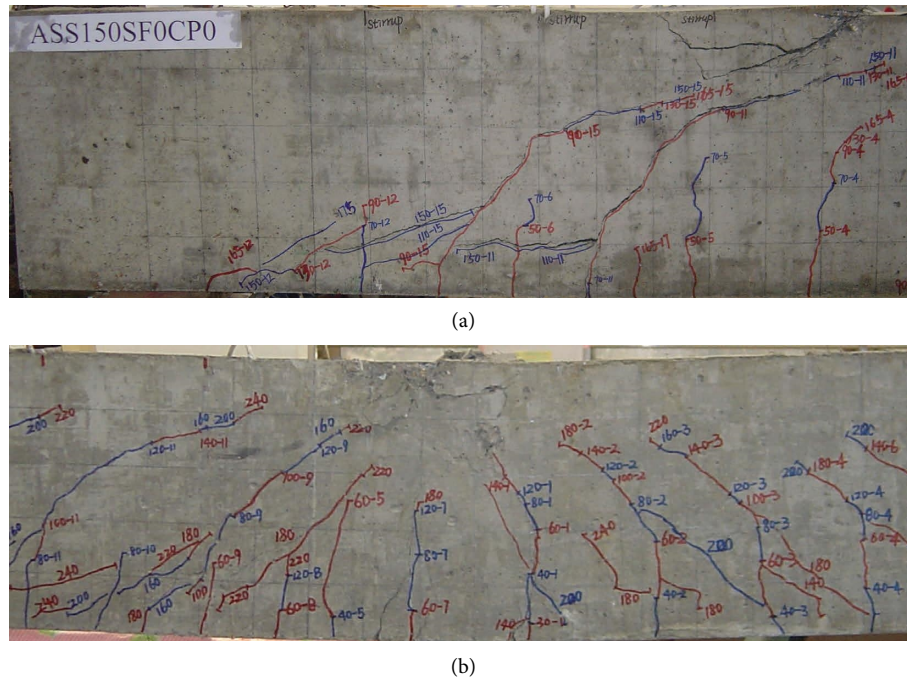
(a)

(b)

FIGURE 8: Crack pattern and failure mode of beams BSS150SF0PF0 and BSS150SF40PF4. (a) Shear failure and crack pattern of beam BSS150SF0PF0. (b) Flexure failure and crack pattern of beam BSS150SF40PF4.

FIGURE 9: Pulling out of steel fiber and breaking down of plastic fibers in hybrid fiber-reinforced RC beam.

The parameter α_1 refers to the slope of the first linear curve, while the parameter α_2 represents that of the second curve. The parameter b_2 is Y-intercept of the second curve. These three parameters are determined by inverse analysis, and the specific values are given in Table 7. Figure 13 compares the experimental and theoretical load-deflection curves of SF20PF6 and SF40PF4, which illustrates that they can fit well.

Then, the ultimate shear loads of beams having hybrid fibers and/or shear reinforcement described in Sections 3.5.1 and 3.5.2 are calculated (Table 8). The average value and coefficient of variation of hybrid fiber-reinforced SCC beams are listed in Table 8.

Although the sample size is small in this paper, some significant results could be obtained. The following can be observed from Figure 8:

(1) The ultimate shear load of beams having hybrid fibers and/or shear reinforcement is predicted by the σ-w and σ-ε design methods.

(2) No matter whether there is a beam with or without shear reinforcement, the forecasted ultimate shear load of the beam is very conservative employing the σ-ε design method.

(3) For the beam without shear reinforcement, the values forecasted by the σ-w design method are close
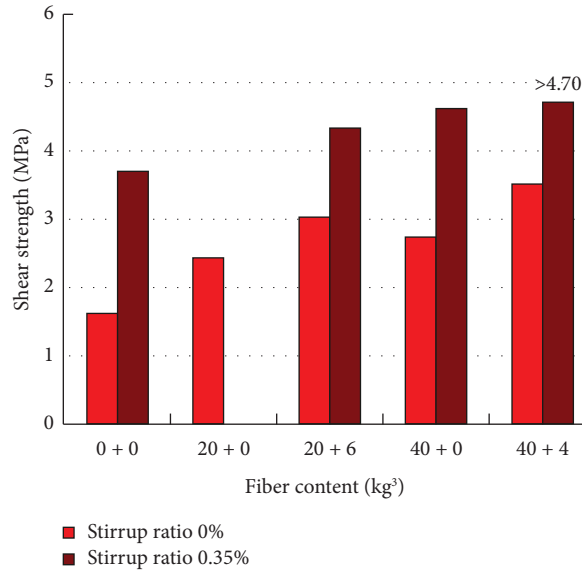
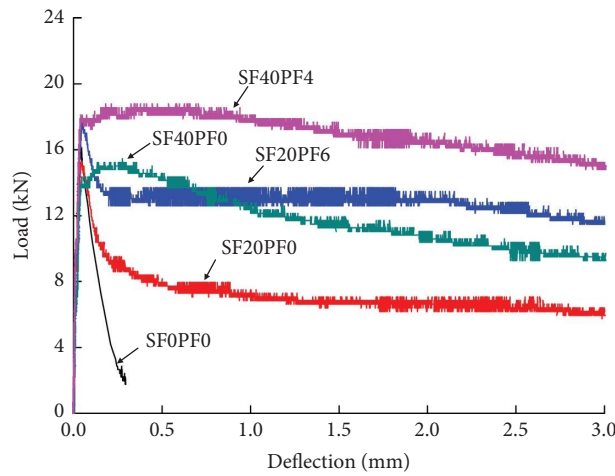FIGURE 10: Shear strength with different fiber dosages.

FIGURE 11: Load-deflection curves of hybrid fiber-reinforced self-consolidating concrete.

TABLE 6: The results of flexural strength and toughness of hybrid fiber-reinforced self-consolidating concrete.

Fiber type	f_L (MPa)	D_c (N·mm)	D_{f2} (N·mm)	D_{f3} (N·mm)	$f_{eq,2}$ (MPa)	$f_{eq,3}$ (MPa)	$f_{R,1}$ (MPa)	$f_{R,2}$ (MPa)	$f_{R,3}$ (MPa)	$f_{R,4}$ (MPa)
SF0PF0	5.17	1.20	—	—	—	—	—	—	—	—
SF20PF0	5.16	0.86	6.41	21.98	4.10	2.81	3.00	2.82	2.69	2.56
SF20PF6	5.04	0.87	8.32	31.20	5.33	3.99	3.79	3.79	3.74	3.66
SF40PF0	5.46	1.01	8.83	34.21	5.65	4.38	3.95	4.10	4.10	4.01
SF40PF4	5.14	0.90	10.06	37.01	6.44	4.74	4.53	4.57	4.47	4.33

to the test values in this paper. On the contrary, those forecasted by the σ-w design method are conservative for the beam containing stirrups.

(4) No matter whether there is a beam with or without shear reinforcement, the mean ratio of the experimental ultimate shear load to the predicted ultimate

shear load and the coefficient of variation using the σ-w design method are better.

It can be concluded that the σ-w design method shows better prediction results in the ultimate shear load having hybrid fibers and/or shear reinforcement compared with the σ-ε design method. However, more experiments should be
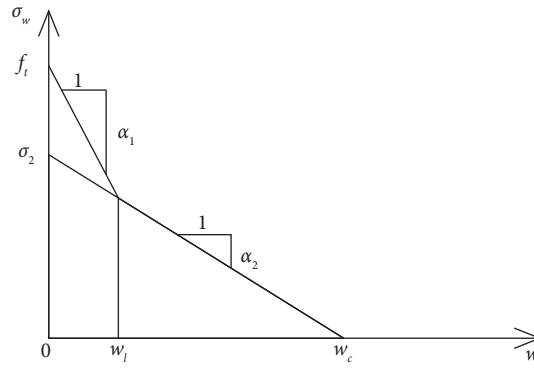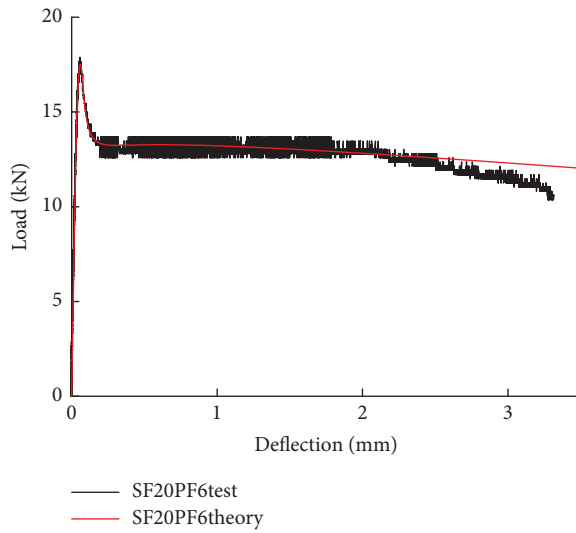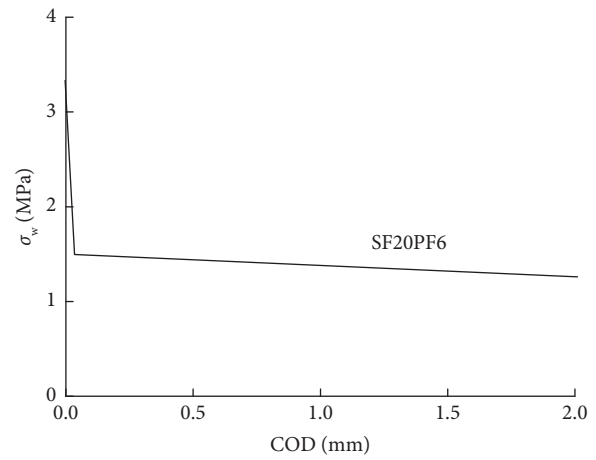
FIGURE 12: Bilinear stress-crack opening relationship.

TABLE 7: The specific values of material parameters of beams.

Fiber type	The values based on inverse analysis		
	α_1	α_2	b_2
SF20PF0	18	0.05	0.29
SF20PF6	13	0.03	0.45
SF40PF0	63	0.19	0.5
SF40PF4	18	0.09	0.59

— SF20PF6test
— SF20PF6theory
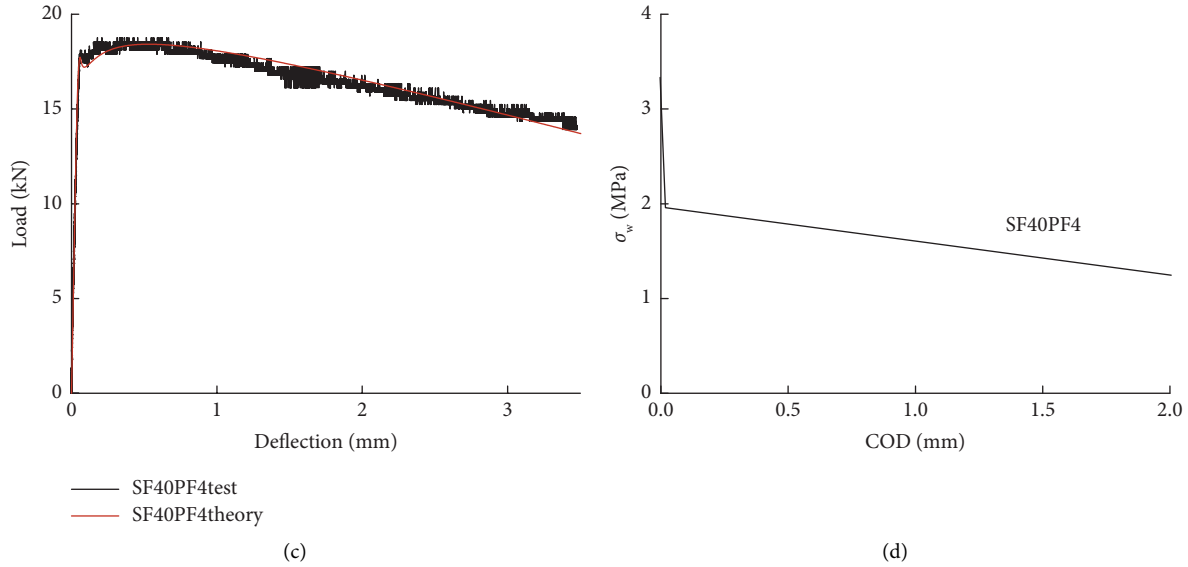
(a)

(b)

FIGURE 13: Continued.

(c)

(d)

FIGURE 13: The evaluation of load-deflection curves concerning the test and theory of beams SF20PF6 and SF40PF4. (a) The evaluation of load-deflection curves concerning test and theory. (b) The tensile stress-crack opening relationship. (c) The evaluation of load-deflection curves concerning test and theory. (d) The tensile stress-crack opening relationship.

TABLE 8: Ultimate shear load, average value, and coefficient of variation of beams.

Fiber type	Test load (kN)	Predicted value of design method (kN)		Test load/predicted value	
		σ-w	σ-ε	σ-w	σ-ε
BSS∞SF0PF0	42.72	35.22	35.22	1.21	1.21
BSS∞SF20PF0	64.58	55.78	46.2	1.16	1.40
BSS∞SF20PF6	80.70	74.59	51.64	1.08	1.56
BSS∞SF40PF0	72.86	65.59	49.27	1.11	1.48
	93.17	73.20	51.12	1.27	1.82
BSS∞SF40PF4			Average	1.17	1.49
			Coefficient of variation	0.066	0.15
BSS150SF0PF0	98.03	65.22	65.22	1.50	1.50
BSS150SF20PF6	115.14	104.59	81.64	1.10	1.41
BSS150SF40PF0	122.87	95.59	79.27	1.29	1.55
BSS150SF40PF4	> 124.74	103.20	81.12	—	—
	111.17	80.23	80.23	1.39	1.39
BSS100SF0PF0			Average	1.32	1.46
			Coefficient of variation	0.13	0.053

tested for verifying the applicability of the σ-w design method.

4. Conclusions

Hybrid fiber-reinforced SCC beams show good mechanical performance, such as crack pattern, shear strength, post-peak bearing capacity, and the possible change of the failure mode of RC rectangular beams, making RC rectangular beams more ductile. The conclusions are as follows:

Hybrid 40.0 kg/m³ steel fiber and 4 kg/m³ plastic fiber can be the upper bound of the fibre content regarding the workability of SCC used in this paper.

Hybrid fibers transform the failure mode of the beam from shear into flexure. BSS150SF0PF0 and BSS100SF0PF0

fail in shear collapse, but BSS150SF40PF4 fails in flexure. Hybrid fibers combined with stirrups illustrate a synergistic response.

When the stirrup ratio remains constant, hybrid fibers enhance the shear strength in contrast to SCC beams without fibers or with only macro-mono-SF.

Better load-carrying capacity and deformability as well as the possible cost benefit of using hybrid fibers can be achieved in terms of shear load-displacement curves, load carrying capacity, and deformability. Hybrids based on macro-SF and PF demonstrate clear synergistic effects.

The σ-w design method can forecast the ultimate shear load containing hybrid fibers and/or shear reinforcement better with satisfactory correlation.

Based on above results, it can be concluded that combining macro-steel fiber and macro-plastic fiber exhibits an extremely positive hybrid effect, and the hybrid fibers can improve the shear resistance of RC rectangular beams.

Data Availability

The data used to support the findings of this study are included within the article.

Conflicts of Interest

The authors declare that there are no conflicts of interest regarding the publication of this paper.

Acknowledgments

References

[1] A. B. Sturm, P. Visintin, and D. J. Oehlers, "Mechanics of shear failure in fiber-reinforced concrete beams," *Journal of Structural Engineering*, vol. 147, no. 3, p. 04020344, 2021.

[2] F. S. Zhang, Y. N. Ding, J. Xu, Y. L. Zhang, W. Q. Zhu, and Y. X. Shi, "Shear strength prediction for steel fiber reinforced concrete beams without stirrups," *Engineering Structures*, vol. 127, pp. 101–116, 2016.

[3] Y. N. Ding, F. S. Zhang, F. Torgal, and Y. L. Zhang, "Shear behaviour of steel fibre reinforced self-consolidating concrete beams based on the modified compression field theory," *Composite Structures*, vol. 94, no. 8, pp. 2440–2449, 2012.

[4] Y. N. Ding, Z. G. You, and S. Jalali, "The composite effect of steel fibres and stirrups on the shear behaviour of beams using self-consolidating concrete," *Engineering Structures*, vol. 33, no. 1, pp. 107–117, 2011.

[5] E. O. Lantsoght, "How do steel fibers improve the shear capacity of reinforced concrete beams without stirrups?" *Composites Part B: Engineering*, vol. 175, p. 107079, 2019.

[6] X. Y. Chen, Y. N. Ding, and C. Azevedo, "Combined effect of steel fibres and steel rebars on impact resistance of high performance concrete," *Journal of Central South University*, vol. 18, no. 5, pp. 1677–1684, 2011.

[7] Y. Y. Lu, N. Li, S. Li, and H. J. Liang, "Experimental investigation of axially loaded steel fiber reinforced high strength concrete-filled steel tube columns," *Journal of Central South University*, vol. 22, no. 6, pp. 2287–2296, 2015.

[8] S. Gali and K. Subramaniam, "Shear behavior of slender and non-slender steel fiber-reinforced concrete beams," *ACI Structural Journal*, vol. 116, no. 3, 2019.

[9] C Cucchiara, L Mendola, and M Papia, "Effectiveness of stirrups and steel fibres as shear reinforcement," *Cement and Concrete Composites*, vol. 26, no. 7, pp. 777–786, 2004.

[10] Y. K. Kwak, M. O. Eberhard, and W. S. Kim, "Shear strength of steel fiber-reinforced concrete beams without stirrups," *ACI Structural Journal*, vol. 99, no. 4, pp. 530–537, 2022.

[11] Y. N. Ding, Y. L. Zhang, and A. Thomas, "The investigation on strength and flexural toughness of fibre cocktail reinforced self-compacting high performance concrete," *Construction and Building Materials*, vol. 23, no. 1, pp. 448–452, 2009.

[12] K. Noghabai, "Beams of fibrous concrete in shear and bending: experiment and model," *Journal of Structural Engineering*, vol. 126, no. 2, pp. 243–251, 2000.

[13] Y. Y. Ding, S. G. Liu, Y. Y. Zhang, and A. Thomas, "The investigation on the workability of fibre cocktail reinforced self-compacting high performance concrete," *Construction and Building Materials*, vol. 22, no. 7, pp. 1462–1470, 2008.

[14] T. Greenough and M. Nehdi, "Shear behavior of fiber-reinforced self-consolidating concrete slender beams," *ACI Materials Journal*, vol. 105, no. 5, pp. 468–477, 2008.

[15] in*National Standard of the People's Republic of China (2010) GB 50010-2010. Code for Design of Concrete Structures*China Architecture & Building Press, Beijing, China, 2010.

[16] National Standard of the People's Republic of China, *Test Methods of Concrete Structures*China Architecture & Building Press, Beijing China, 1992.

[17] Y. Y. Ding, Y. Y. Wang, X. J. Dong, and J. X. Zhang, "An investigation on the workability of fiber reinforced self-compacting high performance concrete," *China Civil Engineering Journal*, vol. 38, no. 11, pp. 51–57, 2005.

[18] EFNARC, *Specification and Guidelines for Self-Compacting Concrete*, The SCC European Project Group, EFNARC, United Kingdom, 2002.

[19] EFNARC, *The European Guidelines for Self-Compacting Concrete Specification, Production and Use*, The SCC European Project Group, EFNARC, United Kingdom, 2005.

[20] H. H. Abrishami and D. Mitchell, "Influence of steel fibers on tension stiffening," *ACI Structural Journal*, vol. 94, no. 6, pp. 769–776, 1997.

[21] RILEM TC 162-TDF, "Final recommendation of RILEM TC 162-TDF: test and design methods for steel fibre reinforced concretesigma-epsilon-design method," *Materials and Structures*, vol. 36, no. 262, pp. 560–567, 2003.

[22] Z. G. You, X. G. Wang, G. H. Liu, H. B. Chen, and S. X. Li, "Shear behaviour of hybrid fibre-reinforced SCC T-beams," *Magazine of Concrete Research*, vol. 69, no. 18, pp. 919–938, 2017.

[23] Z. G. You, Y. L. Zhou, L. C. Yang, and P. Wang, "Experimental study on the shear behavior of fiber reinforced self-compacting concrete rectangular beams," *Advanced Materials Research*, vol. 934, pp. 65–70, 2014.